

Luminescent Color Image Generation on Porous Silicon

Vincent V. Doan and Michael J. Sailor*

Black and white images were projected onto *n*-type silicon (100) wafers during a photoelectrochemical etch to produce a color image that photoluminesces. The photoluminescence originates from a thin layer of luminescent porous silicon that is produced in the photoetch, and the colors that appear in the etched image arise from thin-film optical interference. A diffraction grating was also photoetched into the substrate, demonstrating simultaneous encoding of a gray-scale image into thin-film interference, luminescence, and diffraction phenomena.

Recent studies have shown that an electrochemical etch of Si produces a micro-porous material that photoluminesces in the visible region of the electromagnetic spectrum (1-3). This photoluminescence (PL) has been attributed to quantum confinement effects arising from isolated, nanometer-sized Si features produced during the etch process (1-5), although the origin of PL in porous Si is still under debate (6-9). The striking luminescence of this material has generated a great deal of interest because of the unique role that Si plays in modern electronics technology.

Photoluminescent porous Si can be produced in patterns on a Si wafer by etching the wafer while a binary test pattern is projected onto it (10). Here, we demonstrate that polycontrast images can also be replicated (11) and that the variation in light intensity translates into a variation in etch rates at the Si electrode. This procedure produces two phenomena: first, the etched image appears with false colors under incandescent or fluorescent lights because of thin-film optical interference effects and, second, the image photoluminesces with different emission energies at different spots. The variation in PL energy across the image depends on the photocurrent that existed at each particular location on the wafer during the etch. In addition, photoetching a grid or multiline pattern generates a three-dimensional diffraction grating, which suggests that holographic information can also be stored in this process. These results demonstrate three separate and simultaneous methods of image storage on a Si substrate, all of which may be applicable to optical and holographic display, waveguide, or data storage technologies.

Single-crystal, polished (100) wafers of P-doped (*n*-type) Si of 0.517 ohm-cm resistivity were cut into rectangles with areas of approximately 0.5 cm². We ohmically con-

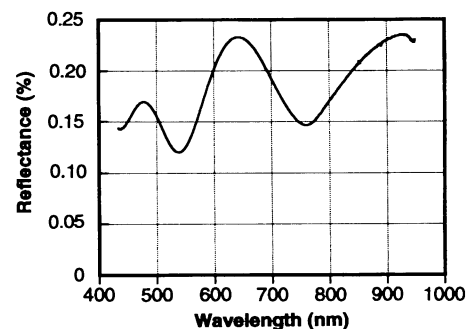
tacted these on the back by scratching with Ga/In eutectic and affixing a Cu wire with Ag print. The entire contact was coated with epoxy, and the resulting device was used as the working electrode in a two-electrode electrochemical cell. A Pt flag with a press-contacted Pt wire attached was used as the counter electrode. The etching bath was a 50:50 (by volume) solution of aqueous 49% HF (Fischer Scientific, electronic grade) and 95% ethanol (Quantum Chemical). Photolithographic etching was carried out in optical-quality plastic cuvettes, and black and white polycontrast images were projected onto the Si samples with a 300-W EXR-type tungsten lamp (filtered through a 450-nm, 20-nm band-pass interference filter) and a reducing lens. The image we used, taken from a dollar note (U.S. currency), is a gray-scale image that also contains periodic line and grid patterns. The samples were etched galvanostatically with a model 363 potentiostat/galvanostat (Princeton Applied Research). Luminescent porous Si images resulted after etching at approximate (average) current densities of 100 $\mu\text{A cm}^{-2}$ for 30 min.

Fig. 1. White-light (A) and fluorescence (B) microscope photographs of an image etched onto *n*-Si. In (B), the fluorescence was excited with a UV lamp (Mineralight UVS-II; Ultraviolet Products, San Gabriel, California) and observed through a 450-nm cutoff filter so that only the red-orange photoluminescence from porous Si was seen.

Fig. 2. Reflectance spectrum from a small spot on a porous Si image. The source (300-W tungsten lamp) and detector (Princeton Instruments charge-coupled device photodetector/Acton Research 0.25-m monochromator) angles were at 45° with respect to the surface normal. The reflectance data are presented as the percentage of light intensity reflected from the sample, relative to a polished, single-crystal Si wafer.

The images generated on the *n*-Si wafers appeared colored under white-light illumination as a result of thin-film interference effects (Fig. 1A) (12). The reflectance spectrum of a small spot on the image (Fig. 2) corresponds to an effective optical thickness (13) of 950 nm, which corresponds to the thickness of the porous Si layer as measured by cross-sectional scanning electron microscopy (1000 nm).

The images appeared red-orange under ultraviolet (UV) irradiation because of luminescence from the porous Si layer (Fig. 1B). Photoluminescence spectra taken at different spots on the porous Si surface had different energy maxima (Fig. 3); the higher energy spectra came from spots that were



Department of Chemistry, University of California, San Diego, La Jolla, CA 92093.

*To whom correspondence should be addressed.

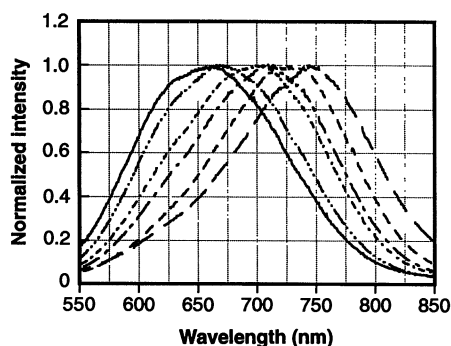


Fig. 3. Photoemission spectra from various spots on the etched image. The spectra were obtained with an expanded He/Cd laser (442 nm, $\sim 0.5 \text{ mW cm}^{-2}$) excitation source and a Princeton Instruments charge-coupled device photodetector/Acton Research 0.25-m monochromator fitted with a fiber optic and microscope objective lens to allow detection from small ($< 1 \text{ mm}^2$) sample areas.

more brightly illuminated during the photoelectrochemical etch. The same variations were seen on wafers with porous Si layers that were too thick to display the optical interference phenomena.

Thus, the shift in wavelength maximum (λ_{max}) can be attributed to variations in the inherent emissive properties of the porous Si. The PL emission maximum on porous Si depends on the etch rate used in the electrochemical etch (14). Because the photocurrent at *n*-Si is proportional to light intensity (15), the intensity variation across the projected image translates into a variation in the etch rate, which presumably leads to the different emission maxima observed. The correlation of the PL λ_{max} to photoetch light intensity was confirmed in separate measurements with the use of uniform photoetch illumination. The value of λ_{max} ranged from 710 to 640 nm for photoetch light intensities ranging from 3×10^{14} to $12 \times 10^{14} \text{ photon cm}^{-2} \text{ s}^{-1}$. The emission maxima were also sensitive to the etch duration and current densities used. In our experiments, the etching time was 30 min at a current density of $100 \mu\text{A cm}^{-2}$.

The background in the picture that we used included a grid pattern. At the reduction ratios used, the replica of the grid produced on the *n*-Si substrate contained 20 lines per millimeter in each direction. Illumination of this area with a He/Ne laser generated a diffraction pattern. The spot spacing matched that predicted from the grating equation for Fraunhofer diffraction (16) and corresponded to a line separation on the *n*-Si substrate of 50 μm . Profilometry measurements (Dektak 3030) showed no height modulation (less than $\pm 20 \text{ nm}$) on the porous Si layer, which indicates that the surface of the etched grating was relatively flat. Because the porosity of anodized porous Si depends on etch current density

(17, 18), the observed diffraction presumably resulted from a periodic density (and refractive index) variation within the etched wafer. This morphology differs from that of conventional ruled gratings, which consist of mechanically imprinted grooves on a surface.

REFERENCES AND NOTES

1. L. T. Canham, *Appl. Phys. Lett.* **57**, 1046 (1990).
2. V. Lehmann and U. Gosele, *ibid.* **58**, 856 (1991).
3. A. G. Cullis and L. T. Canham, *Nature* **353**, 335 (1991).
4. A. Bsiey et al., *Surf. Sci.* **254**, 195 (1991).
5. L. T. Canham, M. R. Houlton, W. Y. Leong, C. Pickering, J. M. Keen, *J. Appl. Phys.* **70**, 422 (1991).
6. S. M. Prokes, O. J. Glembocki, V. M. Bermudez, R. Kaplan, paper presented at the fall meeting of the Materials Research Society, Boston, MA, 2-6 December 1991.
7. Y. H. Xie, W. L. Wilson, F. M. Ross, J. A. Mucha, E. A. Fitzgerald, paper presented at the fall meeting of the Materials Research Society, Boston, MA, 2-6 December 1991.
8. M. S. Brandt, H. D. Fuchs, M. Stutzmann, J. Weber, M. Cardona, *Solid State Commun.* **81**, 307 (1992).
9. R. P. Vasquez, R. W. Fathauer, T. George, A. Ksendzov, T. L. Lin, *Appl. Phys. Lett.* **60**, 1004 (1992).
10. V. V. Doan and M. J. Sailor, *ibid.*, p. 619.
11. Several methods that take advantage of semiconductor photochemistry or photoelectrochemistry have been devised to generate either permanent or temporary images at a semiconductor surface (19-24).
12. E. Hecht, *Optics* (Addison-Wesley, Reading, MA, 1987), pp. 333-378.
13. K. L. Chopra and I. Kaur, *Thin Film Device Applications* (Plenum, New York, 1983), pp. 55-58.
14. N. Koshida and H. Koyama, *Jpn. J. Appl. Phys.* **30**, L1221 (1991).
15. N. S. Lewis, *J. Electrochem. Soc.* **131**, 2496 (1984).
16. M. Born and E. Wolf, *Principles of Optics* (Pergamon, Oxford, 1970), pp. 401-411.
17. G. Bomchil, A. Halimaoui, R. Herino, *Appl. Surf. Sci.* **41-42**, 604 (1989).
18. R. Herino, G. Bomchil, K. Barla, C. Bertrand, J. L. Ginoux, *J. Electrochem. Soc.* **134**, 1994 (1987).
19. R. M. Osgood, A. Sanchez-Rubio, D. J. Ehrlich, V. Daneu, *Appl. Phys. Lett.* **40**, 391 (1982).
20. T. Inoue, A. Fujishima, K. Honda, *J. Electrochem. Soc.* **127**, 1582 (1980).
21. R. H. Micheels, A. D. Darrow, R. D. Rauh, *Appl. Phys. Lett.* **39**, 418 (1981).
22. R. D. Rauh and R. A. LeLievre, *J. Electrochem. Soc.* **132**, 2811 (1985).
23. T. L. Rose, D. H. Longendorfer, R. D. Rauh, *Appl. Phys. Lett.* **42**, 193 (1983).
24. J. D. Venables and R. M. Broudy, *J. Appl. Phys.* **30**, 1110 (1959).

5 March 1992; accepted 8 May 1992

Energetics of Large Fullerenes: Balls, Tubes, and Capsules

Gary B. Adams, Otto F. Sankey,* John B. Page, Michael O'Keeffe, David A. Drabold

First-principles calculations were performed to compare the energies of 29 different fullerene structures, with mass number from 60 to 240, and of eight nonhelical graphite tubes of different radii. A quantity called the planarity, which indicates the completeness of the π -bonding, is the single most important parameter determining the energetics of these structures. Empirical equations were constructed for the energies of nonhelical tubes and for those fullerene structures that may be described as balls or capsules. For a given mass number, ball-shaped fullerenes are energetically favored over capsular (tube-like) fullerenes.

The discovery and practical synthesis (1, 2) of C_{60} has prompted the search for other fullerene-like molecules and other novel forms of carbon. Lamb et al. (3) have created samples containing a wide variety of large carbon fullerenes of mass number up to 290. Scanning tunneling microscope images have shown that the molecules in these samples are exclusively ball-shaped. Graphitic tubes (4, 5) and fullerene capsules (6) are other forms that have been proposed and imaged. At present, there are no simple yet reliable estimates for

the energies of these various structures.

In this report we present computations of the equilibrium configurations and compare the energies of three different types of carbon structures: fullerene balls, graphitic tubes, and fullerene capsules (a tube with ball-like caps). In these computations we used quantum molecular dynamics (QMD) (7-9) simulations. Thirty-seven different structures were simulated, and from these ab initio results we created simple empirical formulas for predicting the energy of any size fullerene ball, tube, or capsule. These empirical formulas are based on only one parameter, the "planarity," which is defined from the π -bonding angle (π angle, or ϕ_{π}). The energetic effect of the size of the HOMO-LUMO gap (highest occupied and lowest unoccupied molecular orbitals) was found to be of secondary importance. For a fixed number of atoms, fullerene balls are

G. B. Adams, O. F. Sankey, J. B. Page, Department of Physics and Astronomy, Arizona State University, Tempe, AZ 85287.

M. O'Keeffe, Department of Chemistry, Arizona State University, Tempe, AZ 85287

D. A. Drabold, Department of Materials Science and Engineering, University of Illinois, Urbana, IL 61801.

*To whom correspondence should be addressed.